

Nonlinear Rabi oscillations in a Bose-Einstein condensate

Nikolay N. Rosanov*

Vavilov State Optical Institute, St. Petersburg, 199053, Russia;

St. Petersburg National Research University of Information Technologies, Mechanics and Optics, St. Petersburg, 197101, Russia;
and Ioffe Physical Technical Institute, 194021, Saint Petersburg, Russia

(Received 17 May 2013; revised manuscript received 13 November 2013; published 10 December 2013)

For a Bose-Einstein condensate in a trap with oscillating barriers, in the resonance approximation, evolution equations are derived. Their analytical solution reveals the existence of two fundamentally different types of nonlinear conservative Rabi oscillations: (i) with periodic temporal variation of moduli and phase difference of levels' amplitudes of probability, and (ii) with monotonic temporal variation of the phase difference. It is shown that the two types can be realized for the same parameters of the scheme, but for different initial conditions. Analytical predictions are confirmed by numerical solution to the Gross-Pitaevskii equation.

DOI: 10.1103/PhysRevA.88.063616

PACS number(s): 03.75.-b

I. INTRODUCTION

The Rabi oscillations, i.e., periodic oscillations of populations of quantum systems resonantly excited by periodic external signal, belong to fundamental quantum-mechanical phenomena; they have been intensively studied for atomic systems [1], in quantum optics [2], for bulk semiconductors and quantum wells and dots [3], graphene [4], spasers [5], Bose-Einstein condensates (BECs) [6], and their hybrids with superconducting quantum interference devices [7]. In the simplest case of two-level atomic systems these oscillations are characterized by the Rabi frequency which is fully determined by the two-level transition dipole moment, the amplitude of the external signal, and detuning between the transition frequency and frequency of the signal. Consequently, the Rabi frequency does not depend on the system's initial conditions. In this regard, it describes the response of a *conservative linear* quantum system to periodic perturbations.

This paper considers the nonlinear coherent Rabi oscillations in an atomic BEC in a dynamical trap. The trap can be organized on the basis of an optical trap formed by the interference of a laser beam incident on a movable mirror with the beam reflected from the mirror [8]. Such a trap provides simultaneous particles' localization and excitation. This is simply an example of resonance excitation of a *conservative nonlinear quantum system* demonstrating some general features of the nonlinear Rabi oscillations; see also Refs. [9,10]. Probably, the most striking of these features is the possibility of formation of fundamentally different dynamical regimes for the same scheme's parameters, but different initial conditions, as shown below.

As a preliminary step, in Sec. II presented are states with definite *quasienergy* [11] of a single quantum particle in an infinite potential well with oscillating positions of barriers, following Ref. [12]. Next, in Sec. III the results of Sec. II are reformulated in terms of evolution equations for probability amplitudes of two levels, both for single quantum particles and for BEC. Their analytical solution is given in Sec. IV. In the main section, Sec. V, an analysis is presented of the *phase plane* demonstrating various regimes of nonlinear Rabi

oscillations for the cases of small and large detunings between the frequency of two-level transition and the frequency of mirror position modulation. In Sec. VI numerical solution to the Gross-Pitaevskii equation is presented and compared with the analytical treatment. General discussion is given in Sec. VII.

II. GOVERNING EQUATIONS AND QUASIENERGIES

For a single quantum particle in a one-dimensional (1D) trap, the wave function $\psi(x,t)$ obeys the Schrödinger equation,

$$i\hbar \frac{\partial \psi}{\partial t} = -\frac{\hbar^2}{2m_p} \frac{\partial^2 \psi}{\partial x^2} + U(x,t)\psi, \quad (1)$$

with the coordinate x , time t , the reduced Planck constant \hbar , the particle mass m_p , and the trap potential U . Though the concrete form of the potential is not critical for the final results, let us assume that it corresponds to the infinite potential well with oscillating barriers. Then the potential $U(x,t) = 0$ for $L_{\text{left}}(t) < x < L_{\text{right}}(t)$, and the boundary conditions for Eq. (1) are

$$\psi(x = L_{\text{left}}(t), t) = 0, \quad \psi(x = L_{\text{right}}(t), t) = 0. \quad (2)$$

The probability to find a particle in the trap, or the wavefunction norm,

$$N_s = \int_{L_{\text{left}}(t)}^{L_{\text{right}}(t)} |\psi(x,t)|^2 dx, \quad (3)$$

according to Eq. (1), does not depend on time. For definiteness, suppose that the left barrier is motionless, $L_{\text{left}}(t) = 0$, and the right barrier oscillates harmonically with period T , frequency $\Omega = 2\pi/T$, and small modulation depth $\mu \ll 1$:

$$L_{\text{right}}(t) = w(t) = L_0[1 + \mu \cos(\Omega t)]. \quad (4)$$

For $\mu = 0$ eigensolutions of Eq. (1) have a discrete highly nonequidistant spectrum:

$$\psi_n^{(0)}(x,t) = e^{-i\frac{E_n^{(0)}}{\hbar}t} \sin(k_n^{(0)}x), \quad k_n^{(0)} = \frac{\pi n}{L_0}, \quad (5)$$

$$E_n^{(0)} = \frac{\hbar^2}{2m_p} k_n^{(0)2} = \frac{\pi^2 \hbar^2}{2m_p L_0^2} n^2, \quad n = 1, 2, 3, \dots$$

*nrosanov@yahoo.com

Unperturbed eigenfunctions $\psi_n^{(0)}$ are the even (odd) functions of $(x - L_0/2)$ for an odd (even) n .

States with fixed quasienergy [11] are determined by the conditions,

$$\psi_\varepsilon(x, t) = u_\varepsilon(x, t)e^{-i\frac{\varepsilon}{\hbar}t}, \quad u_\varepsilon(x, t + T) = u_\varepsilon(x, t). \quad (6)$$

For the problem under consideration these states were found in [12]. The Fourier series for the periodic functions of time $u_\varepsilon(x, t)$ are

$$u_\varepsilon(x, t) = \sum_{l=-\infty}^{\infty} a_l \chi_{\varepsilon, l}(x) e^{-il\Omega t}. \quad (7)$$

Then

$$\chi_{\varepsilon, l}(x) = \begin{cases} \sin(k_{\varepsilon, l}x), & \varepsilon + \hbar\Omega l > 0, \\ \sinh(k_{\varepsilon, l}x), & \varepsilon + \hbar\Omega l < 0, \end{cases} \quad (8)$$

where $k_{\varepsilon, l} = \sqrt{2m_p|\varepsilon + \hbar\Omega l|/\hbar}$. In this case the Schrödinger equation, Eq. (1), and the boundary condition at $x = 0$ are satisfied automatically. Equation (2) at the oscillating boundary gives

$$\sum_{l=-\infty}^{\infty} a_l \chi_{\varepsilon, l} \{L_0[1 + \mu \cos(\Omega t)]\} e^{-il\Omega t} = 0. \quad (9)$$

Let us decompose the periodic functions of time $\chi_{\varepsilon, l}$ to the Fourier series,

$$\chi_{\varepsilon, l} \{L_0[1 + \mu \cos(\Omega t)]\} = \sum_{p=-\infty}^{\infty} F_{l, p}(\varepsilon) e^{ip\Omega t}, \quad (10)$$

where $F_{l, p}(\varepsilon) = F_{l, -p}(\varepsilon)$. Then it follows from Eq. (9) that

$$\sum_{l=-\infty}^{\infty} F_{l, q+l}(\varepsilon) a_l = 0, \quad q = 0, \pm 1, \pm 2, \dots \quad (11)$$

This is an infinite homogeneous system of linear algebraic equations with respect to coefficients a_l . The equation for determination of quasienergy spectrum ε coincides with the condition of vanishing of this system's determinant. For small μ , the quasienergy is close to the corresponding unperturbed eigenenergy $E_n^{(0)}$:

$$\varepsilon = E_n^{(0)} + \delta\varepsilon, \quad |\delta\varepsilon| \ll E_n^{(0)}. \quad (12)$$

Here of interest is the resonant case, when the modulation frequency Ω is close to the frequency of transition between the two levels n and m :

$$\hbar\Omega = E_m^{(0)} - E_n^{(0)} + \hbar\delta\Omega, \quad |\delta\Omega|/\Omega \ll 1. \quad (13)$$

Then, for small μ , only the amplitudes with $l = n$ and m can be sufficiently large. It corresponds to the two-level approximation widely used in quantum mechanics and quantum optics; see, e.g., [1]. In the case considered, the resonance approximation is based on the nonparabolic shape of trap potential with highly nonequidistant energy levels in the zero-order approximation [see Eq. (5)]. According to Eq. (13), the modulation frequency Ω differs from the frequency of transition, between levels n and m by the value of the order of the theory small parameter μ . If only level n , e.g., the ground level, is occupied initially, then, due to the modulation, two “resonant” levels n and m will have substantial population

whereas population of other levels will be of the order μ^2 . If some other levels are excited initially, then they would not be connected with the “resonant” levels by the modulation and therefore would have the trivial dynamics. Now Eq. (11) for the “resonant” levels reads

$$F_{nn}a_n + F_{mm}a_m = 0, \quad F_{nm}a_n + F_{mn}a_m = 0, \quad (14)$$

with

$$F_{nn} = (-1)^n \frac{n\pi}{2} \frac{\delta\varepsilon}{E_n^{(0)}}, \quad F_{nm} = (-1)^n \frac{\mu}{2} n\pi, \quad (15)$$

$$F_{mn} = (-1)^m \frac{m\pi}{2E_m^{(0)}} (\delta\varepsilon + \hbar\delta\Omega), \quad F_{mm} = (-1)^m \frac{\mu}{2} N\pi.$$

The determinant of the system (14) turns to zero for

$$\delta\varepsilon_{(\pm)} = -\frac{\hbar\delta\Omega}{2} \pm \sqrt{\left(\frac{\hbar\delta\Omega}{2}\right)^2 + \mu^2 E_n^{(0)} E_m^{(0)}}. \quad (16)$$

The equation above describes the quasienergy splitting and corresponding Rabi oscillations with the frequency $\Omega_R = \sqrt{\delta\Omega^2 + 4\mu^2 E_n^{(0)} E_m^{(0)}/\hbar^2}$ and period $T_R = 2\pi/\Omega_R$ typical of two-level schemes' resonant excitation [13].

III. EVOLUTION EQUATIONS

An equivalent description of the Rabi oscillations can be given by the evolution equations for amplitudes $a_{n, m}$. For this goal, let us replace the quasienergy shift $\delta\varepsilon$ by the operator $i\hbar \frac{d}{dt}$ in Eq. (15). Then Eq. (14) reads

$$i\hbar \frac{da_n}{dt} + (-1)^{m-n} \mu n m E_m^{(0)} a_m = 0, \quad (17)$$

$$i\hbar \frac{da_m}{dt} + (-1)^{m-n} \mu n m E_m^{(0)} a_n + \hbar\delta\Omega a_m = 0.$$

If one seeks the solution to Eq. (17) in the form of $a_{n, m}(t) = a_{n, m} e^{-i(\delta\varepsilon/\hbar)t}$, then one gets Eq. (16). Note also that the amplitudes $a_{n, m}$ are assumed to be slow functions of time in terms of frequencies of transitions between the levels.

Equations (17) are convenient for the generalization for the nonlinear case. In fact, if we consider the atomic Bose-Einstein condensate (BEC) in the dynamic trap, then the macroscopic wave function $\psi(x, t)$ obeys the Gross-Pitaevskii equation (GPE) [14],

$$i\hbar \frac{\partial \psi}{\partial t} = -\frac{\hbar^2}{2m_p} \frac{\partial^2 \psi}{\partial x^2} + U_0 |\psi|^2 \psi. \quad (18)$$

The parameter of nonlinearity U_0 can be positive or negative, depending on the external magnetic field. Now the value N_s in Eq. (3) becomes proportional to the number of atoms in the trap. The GPE is valid for weakly nonideal diluted atomic gases at zero temperature; a similar mean-field equation for exciton condensates in semiconductors is known as the Keldysh equation [15].

As in the previous section, Sec. II, here of interest is also the case of the resonant excitation [see Eq. (13)]. The corresponding nonlinear generalization of Eqs. (17) for BEC

reads

$$\begin{aligned}
 i\hbar \frac{da_n}{dt} + (-1)^{m-n} \mu n m E_m^{(0)} a_m \\
 - U_0 \left(\frac{3}{4} |a_n|^2 + |a_m|^2 \right) a_n = 0, \\
 i\hbar \frac{da_m}{dt} + (-1)^{m-n} \mu n m E_m^{(0)} a_n \\
 + \left[\hbar \delta \Omega - U_0 \left(\frac{3}{4} |a_m|^2 + |a_n|^2 \right) \right] a_m = 0.
 \end{aligned} \tag{19}$$

The validity of the resonance approximation for the diluted atomic BEC describing by the GPE (18) is, as in the previous section, based on the trap potential shape with *highly nonequidistant energy levels*. In fact, in the zero-order approximation when the small nonlinear term can be neglected ($U_0 \rightarrow 0$), Eq. (18) is reduced to the Schrödinger equation (1). Then Eq. (5) gives again the energy of the n th level proportional to n^2 . Correspondingly, the estimations for populations of different levels under resonance modulation presented in the Sec. II retain their validity. Physically it can be explained because, in the Gross-Pitaevskii theory, only weakly nonideal gas is considered with sufficiently small atomic concentration. Note that in the case considered the two-level model is much more accurate than in the case when nonuniform spacing of the levels is due to only nonlinear factors (see, e.g., Ref. [16]). On the same reason, it is not necessary to use here the approach of nonlinear modes [16]. Additionally to the analytical estimations, it will be confirmed by the numerical solution to the GPE in Sec. VI.

Equations (19) describe a conservative system with conservation of the number of particles; see the normalization condition (3) where now

$$N_s = \frac{N_3}{S_0} \approx \frac{1}{2} (|a_n|^2 + |a_m|^2) L_0. \tag{20}$$

Here S_0 is the area of the trap transverse section and N_3 is the total number of particles in the trap with volume $V_0 = S_0 L_0$. In accordance with Eq. (18), Eqs. (19) are invariant to time reversal $t \rightarrow -t$ with simultaneous phase conjugation $a_{n,m} \rightarrow a_{n,m}^*$. For dimensionless values,

$$\begin{aligned}
 \tilde{a}_{n,m} = a_{n,m} \sqrt{\frac{V_0}{2N_3}}, \quad \tilde{t} = t \frac{\mu n m E_m^{(0)}}{\hbar}, \\
 \delta \omega = \frac{\hbar \delta \Omega}{\mu n m E_m^{(0)}}, \quad \nu = \frac{U_0 N_3}{2V_0 \mu n m E_m^{(0)}}.
 \end{aligned} \tag{21}$$

Eqs. (19) read

$$\begin{aligned}
 i \frac{d\tilde{a}_n}{d\tilde{t}} + (-1)^{m-n} \tilde{a}_m - \nu (3|\tilde{a}_n|^2 + 4|\tilde{a}_m|^2) \tilde{a}_n = 0, \\
 i \frac{d\tilde{a}_m}{d\tilde{t}} + (-1)^{n-m} \tilde{a}_n + [\delta \omega - \nu (3|\tilde{a}_m|^2 + 4|\tilde{a}_n|^2)] \tilde{a}_m = 0.
 \end{aligned} \tag{22}$$

The normalization condition (20) gives

$$|\tilde{a}_n|^2 + |\tilde{a}_m|^2 = 1. \tag{23}$$

IV. SOLUTION TO THE EVOLUTION EQUATIONS

Let us introduce real amplitudes and phases,

$$\tilde{a}_{n,m} = A_{n,m} e^{i\varphi_{n,m}}, \quad \Phi = \varphi_m - \varphi_n. \tag{24}$$

Then Eq. (23) takes the form,

$$A_n^2 + A_m^2 = 1. \tag{25}$$

The governing equations for the real amplitude A_n , $0 < A_n < 1$, and phase difference Φ are, with replacing $\tilde{t} \rightarrow t$:

$$\begin{aligned}
 \frac{d\Phi}{dt} = \delta \omega - \nu (2A_n^2 - 1) + (-1)^{m-n} \frac{2A_n^2 - 1}{A_n \sqrt{1 - A_n^2}} \cos \Phi, \\
 \frac{dA_n}{dt} = -(-1)^{m-n} \sqrt{1 - A_n^2} \sin \Phi.
 \end{aligned} \tag{26}$$

This system of equations has an integral of motion,

$$\cos \Phi = \frac{(-1)^{m-n}}{2} \frac{(A_n^2 - C)}{A_n \sqrt{1 - A_n^2}} [(\delta \omega + \nu) - \nu (A_n^2 + C)], \tag{27}$$

with the constant of integration C . With the help of Eq. (27), one can solve the second of Eqs. (26) and find the dependence $A_n(t)$ in terms of elliptic functions, following which, solution to the first of Eqs. (26) gives the analytical form of the dependence $\Phi(t)$. However, it is more instructive to analyze the solutions to Eq. (26) with the help of the phase plane of this system, where they are represented by closed lines (A_n, Φ) . In fact, it is convenient to treat A_n as a polar radius and Φ as a polar angle of the phase plane; see Figs. 1(a) and 2(a) where $X = A_n \cos \Phi$. Trajectories pass through each point of the polar plane inside the circle with the radius $A_n = 1$. At $A_n = 1$ (when only the n th level is occupied) and $A_n = 0$ (when only the m th level is occupied), there are singularities of Eqs. (26). Interestingly, some trajectories correspond to the complex values of the constant of integration C , whereas the values A_n, Φ remain real.

V. PHASE PLANE ANALYSIS

Fixed points of the phase plane can be found when equalizing to zero the right sides of Eqs. (26). Then,

$$\cos \Phi = \pm 1, \tag{28}$$

$$\delta \omega = (2A_n^2 - 1) \left(\nu \mp (-1)^{m-n} \frac{1}{A_n \sqrt{1 - A_n^2}} \right).$$

Exact resonance (detuning $\delta \omega = 0$). In this case, there are two fixed points ($A_n = 2^{-1/2}$, $\Phi = 0$) and ($A_n = 2^{-1/2}$, $\Phi = \pi$) for any value of the nonlinearity parameter ν . Four more fixed points appear for $\nu > 2$; for them $\Phi = 0$ and π and

$$A_n^2 = \frac{1}{2} \left(1 \pm \sqrt{1 - \frac{4}{\nu^2}} \right). \tag{29}$$

Below we will treat only the simpler case of $\nu < 2$ when only two fixed points exist [B and C in Fig. 1(a)]. For $C = 0$ and 1, Eq. (27) reads (for $\delta \omega = 0$)

$$\cos \Phi = (-1)^{N-n} \frac{\nu}{2} A_n \sqrt{1 - A_n^2}. \tag{30}$$

This curve passes through point $A_n = 0$ and ends at points $A_n = 1$, $\Phi = 0$, and π , as shown in Fig. 1(a), (see curve D),

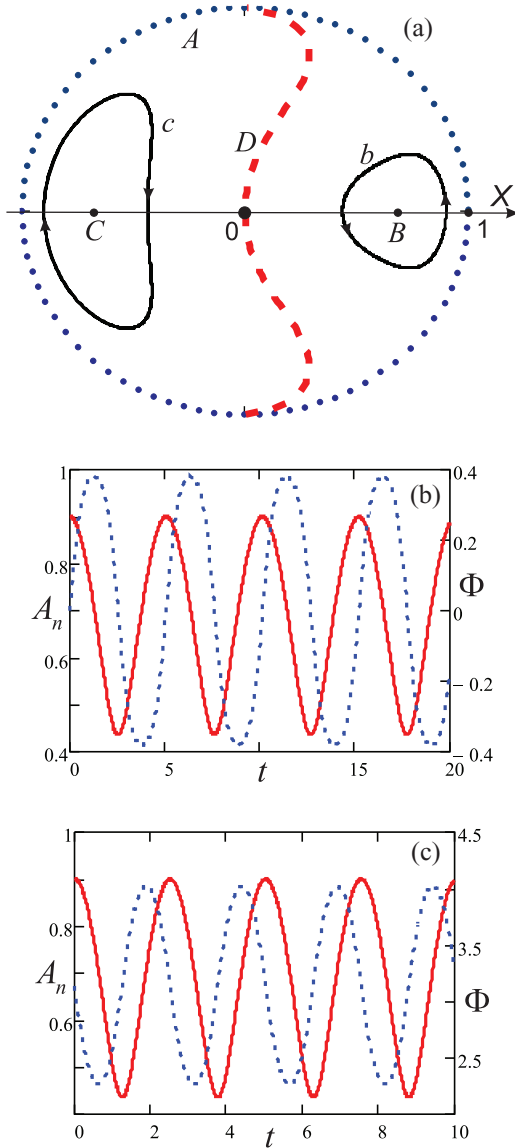


FIG. 1. (Color online) (a) Phase plane for zero detuning, $\delta\omega = 0$, $\nu = 1.5$. The circle A [the dotted (blue) curve], with the center 0 and radius 1, is divided into two cells by the separatrix D [the broken (red) curve]. Each of the two cells contains a fixed point, B in the right cell and C in the left cell. Through any point inside each of the cells, passes one trajectory, a closed curve wraps around the corresponding fixed point. Solid (black) curves with the arrows b and c are examples of these trajectories; the arrows show the direction of time evolution. (b) and (c) Temporal dependencies of the amplitude $A_n(t)$ [solid (red) lines] and the phase difference $\Phi(t)$ [dotted (blue) lines] for the trajectories b and c in Fig. 1(a).

where for definiteness we suppose that n and m are of the same parity. It is a separatrix, because it divides the phase plane into two cells, the right and the left ones in Fig. 1(a). In each cell, trajectories are the closed lines disposed approximately concentrically around the corresponding fixed point: B ($A_n = 2^{-1/2}$, $\Phi = 0$) in the right cell and C ($A_n = 2^{-1/2}$, $\Phi = \pi$) in the left cell. The trajectories correspond to periodic oscillations with time of both the amplitude $A_n(t)$ and the phase difference $\Phi(t)$, as shown in Figs. 1(b) and 1(c). The period of oscillations differs for different trajectories, i.e., it depends on the initial

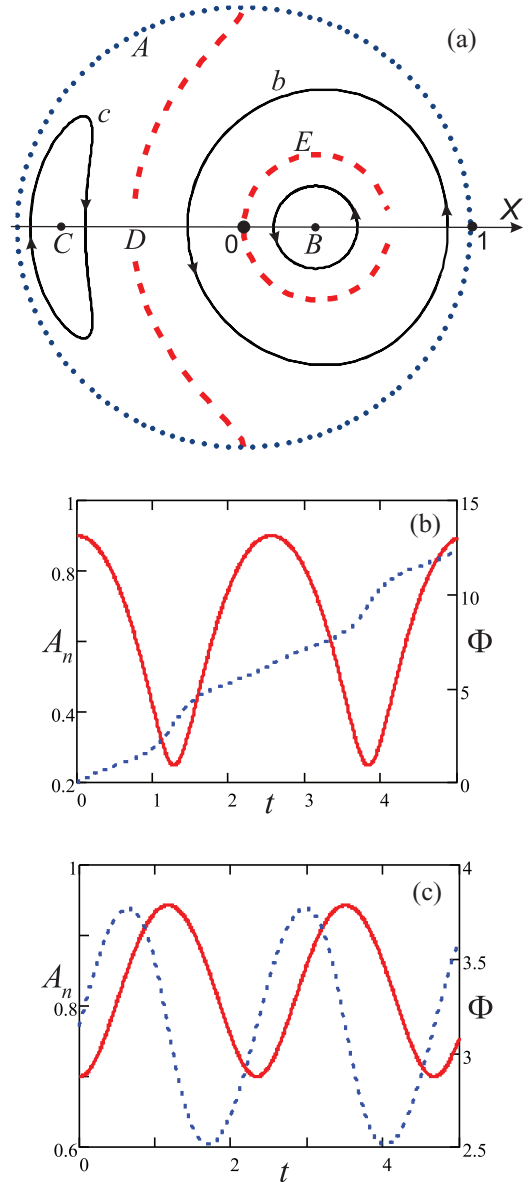


FIG. 2. (Color online) (a) Phase plane for nonzero detuning, $\delta\omega = 1.5$, $\nu = 1.5$. The circle A [the dotted (blue) curve] with the center 0 and radius 1 is divided into three cells by the separatrices D and E [the broken (red) curves]. B and C are fixed points. Through any point inside each of the cells, passes one trajectory, a closed curve of the two types. In the first (second) type, the beginning of coordinates 0 is outside (inside) the curve. The solid (black) curves with the arrows b (the first type) and c (the second type) are examples of these trajectories; the arrows show the direction of time evolution. (b) and (c) Temporal dependencies of the amplitude $A_n(t)$ [solid (red) lines] and the phase difference $\Phi(t)$ [dotted (blue) lines] for the trajectories b and c in Fig. 2(a).

conditions. More exactly, the period decreases (increases) in the right (left) cells when the trajectory departs from the fixed point. The modulation depth is not full, but it approaches to 100% for trajectories near the boundaries of the cells.

Nonzero detuning. Now separatrices corresponding to curves described by Eq. (27) for $C = 0$ and $C = 1$ differ, and the phase plane has a more complicated structure. In Fig. 2,

shown are the results for the fairly large detuning $\delta\omega = 1.5$ and equal parity of states n and m . In Fig. 2(a) the separatrix D ends at points $A_n = 1$, $\Phi = 0$, and π , and the separatrix E is a closed line passing through 0. Now the temporal dependence of the phase difference, $\Phi(t)$, can be of two types, depending on initial conditions: (i) periodic, as in the previous case, and (ii) monotonic which can be decomposed into a sum of a periodic function and a component linear in time. The phase plane is divided into three cells [Fig. 2(a)]. The left cell—a “semimoon”—is bounded by the left semicircle and the separatrix D . It is of the same type as in the previous case, i.e., it consists of closed trajectories wrapping around the fixed point C ($\Phi = \pi$); for trajectories in this cell both the amplitude A_n and the phase difference Φ vary periodically with time (the first type of trajectories). The features of trajectories inside the second separatrix E are the same. However, in the cell bounded by the separatrices D and E and the right semicircle A , trajectories wrap around the beginning of the coordinates 0 and correspond to periodic temporal variation of the amplitude A_n and monotonic variation of the phase difference Φ (the second type of trajectories). These two types of trajectories are illustrated in Figs. 2(b) and 2(c). They are similar to trajectories of a classical pendulum with an angle periodic variation for small initial velocities and a monotonous variation for large velocities.

VI. NUMERICAL SOLUTION TO THE GROSS-PITAEVSKII EQUATION

The problem given by Eq. (18) and Eq. (2) can be reduced to a more tractable case with boundary conditions for fixed interval ends. To this end, let us introduce the coordinate transformation $\{x, t\} \rightarrow \{\xi, \tau\}$ where

$$\begin{aligned} \xi &= L_0 \frac{x - L_{\text{left}}(t)}{w(t)}, \quad \tau = t, \\ w(t) &= L_{\text{right}}(t) - L_{\text{left}}(t). \end{aligned} \quad (31)$$

Then the GPE and the boundary conditions take the form,

$$\begin{aligned} i\hbar \frac{\partial \psi}{\partial \tau} + \frac{\hbar^2}{2m_p} \frac{L_0^2}{w^2(\tau)} \frac{\partial^2 \psi}{\partial \xi^2} - U_0 |\psi|^2 \psi \\ = i\hbar \left[\dot{L}_{\text{left}}(\tau) + \frac{\dot{w}(\tau)}{L_0} \xi \right] \frac{L_0}{w(\tau)} \frac{\partial \psi}{\partial \xi}, \\ \psi(\xi = 0, \tau) = 0, \quad \psi(\xi = L_0, \tau) = 0. \end{aligned} \quad (32)$$

Furthermore, we will treat the case $w(\tau) = L_0 = \text{const}$ because, first, features of nonlinear Rabi oscillations are of general nature not depending on the specific form of the trap dynamics and, second, the corresponding governing equation has in this case a simpler form:

$$i\hbar \frac{\partial \psi}{\partial \tau} + \frac{\hbar^2}{2m_p} \frac{\partial^2 \psi}{\partial \xi^2} - U_0 |\psi|^2 \psi = i\hbar \dot{L}_{\text{left}}(\tau) \frac{\partial \psi}{\partial \xi}. \quad (33)$$

Next, we introduce dimensionless coordinates $x' = \xi/L_0$, $t' = \Omega\tau$, and the specific form of trap dynamics,

$$L_{\text{left}}(t') = \mu \cos \Omega\tau = \mu \cos t'. \quad (34)$$

The final form of the problem is (we replace $x' \rightarrow x$ and $t' \rightarrow t$)

$$\begin{aligned} i \frac{\partial \psi}{\partial t} + a \frac{\partial^2 \psi}{\partial x^2} &= -i\mu \sin(t) \frac{\partial \psi}{\partial x} + s |\psi|^2 \psi, \\ \psi(x = 0, t) &= 0, \quad \psi(x = 1, t) = 0. \end{aligned} \quad (35)$$

Here $a = \hbar/(2m_p L_0^2 \Omega)$. By the appropriate choice of the conservative norm,

$$N_0 = \int_0^1 |\psi(x, t)|^2 dx, \quad (36)$$

one can suppose $s = \pm 1$. The modulation depth μ is assumed to be small, $\mu \ll 1$.

For $\mu = 0$ and $s = 0$ there are solutions to the linear problem in the form,

$$\psi(x, t) = a_1(t) \sin(\pi x) + a_2(t) \sin(2\pi x), \quad (37)$$

where $a_n(t) \sim e^{-i\omega_n t}$, $\omega_n = \pi^2 n^2 a$, $n = 1, 2$. Then the resonance condition is $\omega_2 - \omega_1 = 1$, or $a = a_{\text{res}} = 1/(3\pi^2)$. Therefore we assume $a = qa_{\text{res}}$, $|q - 1| \ll 1$. The initial condition for the nonlinear problem is

$$\psi(x, t = 0) = a_{10} \sin(\pi x) + a_{20} e^{i\Phi_0} \sin(2\pi x). \quad (38)$$

Here constants a_{10} , a_{20} , and Φ_0 are real. The norm, Eq. (36), is $N_0 = (a_{10}^2 + a_{20}^2)/2$.

To compare numerical solution to the GPE with the analytical results, Secs. IV and V, it is necessary to derive from the numerical data two spatial Fourier components,

$$a_n(t) = 2 \int_0^1 \psi(x, t) \sin(\pi n x) dx, \quad n = 1, 2. \quad (39)$$

The approximate norm,

$$N_{12}(t) = \frac{1}{2} (|a_1(t)|^2 + |a_2(t)|^2), \quad (40)$$

should be close to N_0 [Eq. (36)]. The criterion of the two-mode approximation's validity is $|\delta N| \ll N_0$ where $\delta N(t) = N_0 - N_{12}(t)$. In calculations we discretize the coordinate x with step of grid 0.001 or 0.01, reducing Eq. (35) to a set of ordinary differential equations and use the following values of parameters: $s = 1$, $N_0 = 0.01$, $\mu = 0.01$. We will consider cases of exact resonance with $q = 1$ and nonzero detuning, $q = 1.01$. The value of the small parameter in analytics about 0.01 is sufficient for applicability of the analytics presented above, because the criterion of the approximation validity is satisfied then with good precision, $\delta N/N_0 < 0.005$ [see typical examples in Figs. 3(a) and 3(b)]. When comparing numerics with the analytics, note that A_1 and A_n are normalized in different ways and the form of modulation in analytics, Eq. (4), differs from that in numerics, Eq. (34); therefore we check here the correlation of the general, qualitative type of the driven BEC nonlinear dynamics. Let us remind that the analytics in the form presented in Secs. III and IV is applicable and coincides with the numerics with good precision only in the cases of small modulation depth, $\mu \ll 1$, small detunings, $|q - 1| \ll 1$, and weak nonlinearity, $N_0 \ll 1$.

Exact resonance, $q = 1$. Phase plane (A_1, Φ) where $A_1 = |a_1|$ and $\Phi = \text{arg} a_2 - \text{arg} a_1$, for trajectories extracted from numerical simulations is presented in Fig. 4(a); it should be compared with Fig. 1(a) corresponding to the analytics of

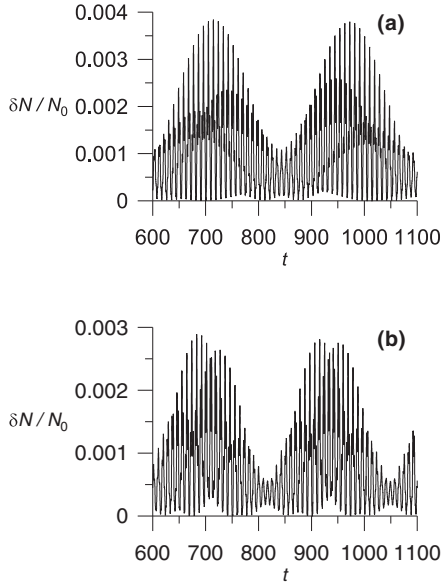


FIG. 3. Temporal dependence of the relative inaccuracy $\delta N(t)/N_0$ for $q = 1$ (a) and $q = 1.01$ (b).

Sec. V. One can see that, as well as in Fig. 1(a), the phase plane is separated into two cells filled with closed trajectories wrapping around two fixed points, one on the positive semiaxis X and the other on the negative semiaxis X . Typical periodic temporal dependencies of amplitude A_1 and phase difference Φ are given in Figs. 4(b) and 4(c); they are similar to those presented in Figs. 1(b) and 1(c). As well as in analytics of Secs. IV and V, the Rabi period T_R is different for different trajectories: $T_R = 220$ for trajectory (1) in Fig. 4(a), 224 for (2), 250 for (3), and 260 for (4).

New features that are beyond the two-mode approximation are the following. First, additionally to a “long period” presented in Figs. 4(b) and 4(c), there is also a “short period” with weak modulation depth, as shown in Fig. 4(d). Due to this additional modulation, trajectories given in Fig. 4(a) have effectively a finite width. The second new feature is due to slight displacement of the separatrix between the two cells from the origin of coordinates. Then even for the exact resonance there is a narrow bundle of trajectories in the left cell with the origin of coordinates inside them. Correspondingly, phase difference varies monotonically with time for them as shown in Fig. 4(e).

Nonzero detuning, $q = 1.01$. Corresponding phase plane given in Fig. 5(a) is similar to the “analytical” one in Fig. 2(a). The phase plane is separated into two cells with trajectories wrapping around two different fixed points. Additionally, trajectories in the right cell are divided in those exterior with respect to the origin of coordinates and those wrapping around it; the former trajectories correspond to periodic temporal variation both of amplitude A_1 and phase difference Φ [Figs. 5(b) and 5(d)], whereas for the latter trajectories phase difference varies with time monotonically [Fig. 5(c)]. Rabi period T_R is again different for different trajectories: $T_R = 213$ for trajectory (1) in Fig. 5(a), 215 for (2), 222 for (3), 231 for (4), and 234 for (5). As well as in the case of exact resonance, there is also additional small-scale temporal

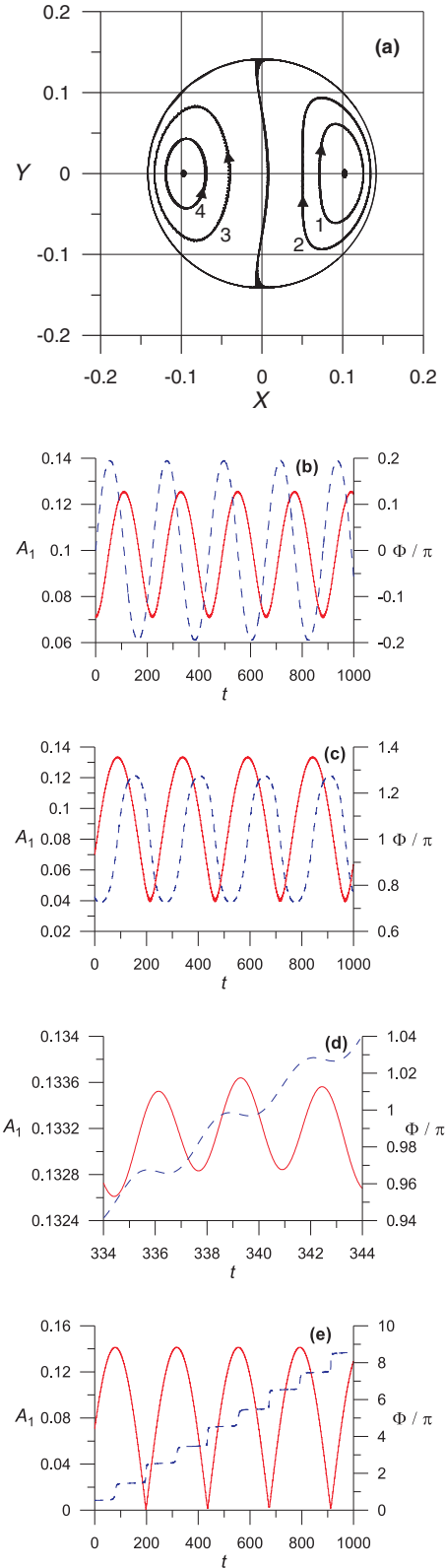


FIG. 4. (Color online) (a) Phase plane for zero detuning found by numerical solution to the Gross-Pitaevskii equation; compare with Fig. 1(a). (b), (c) Dependencies $A_1(t)$ [solid (red) lines] and $\Phi(t)$ [dotted (blue) lines] for trajectories 1 and 3 in (a), correspondingly. (d) Small-scale modulation for trajectory 3 in (a). (e) Example of dynamics with monotonic temporal variation of phase difference $\Phi(t)$ [dotted (blue) lines].

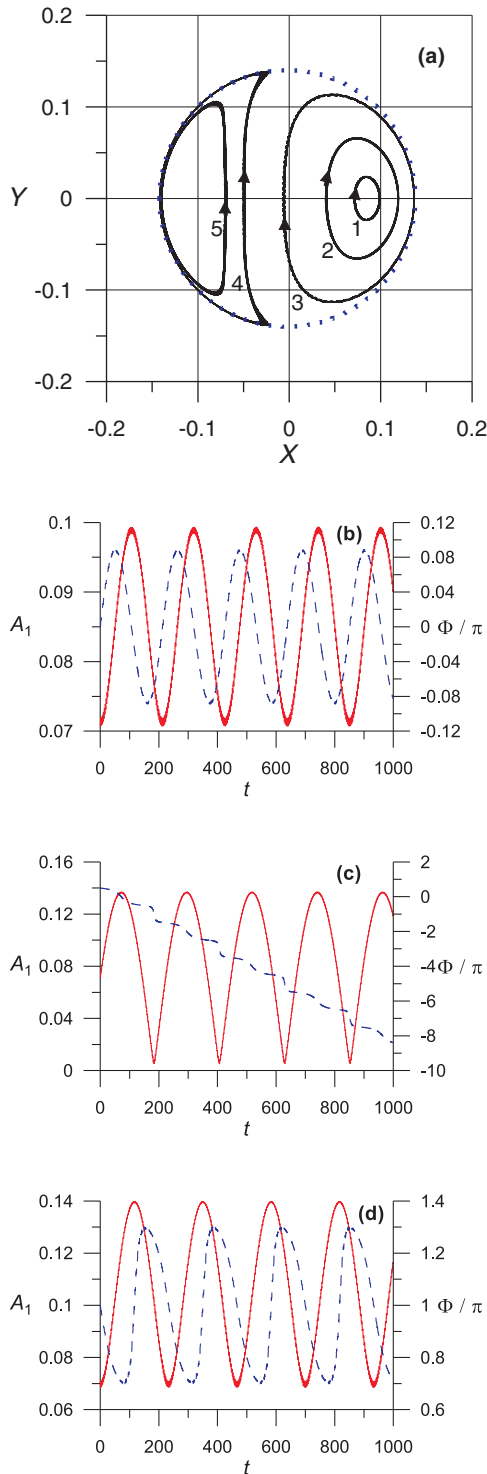


FIG. 5. (Color online) (a) Phase plane for nonzero detuning, $q = 1.01$, found by numerical solution to the Gross-Pitaevskii equation; compare with Fig. 2(a). (b), (c), (d) Dependencies $A_1(t)$ [solid (red) lines] and $\Phi(t)$ [dotted (blue) lines] for trajectories 1, 3, and 5 in (a), correspondingly.

modulation of amplitude A_1 and phase difference Φ not shown here.

VII. DISCUSSION

The analyzed scheme of a dynamic trap, where the trap is used for localization and excitation of BEC simultaneously, can be realized by two counterpropagating laser beams—the incident one and the one reflected from a movable mirror, whose position is modulated. For a trap with the length of $10 \mu\text{m}$, the typical frequency of two-level transition corresponds to the kHz range. Therefore the modulation frequencies necessary for the BEC resonance excitation are in the microwave range convenient for experiments. Obtaining an analytical solution to the nonlinear evolution equations becomes possible due to the conservative nature of the scheme with conservation of the number of BEC atoms in the trap; in this point the nonlinear Rabi oscillations differ radically from those in dissipative schemes with losses and relaxation. The two-mode, or resonance approximation is appropriate due to highly nonequidistant distribution of BEC energy levels in the trap. Numerical solution to the Gross-Pitaevskii equation confirms the analytics and reveals also additional small-scale temporal modulation of BEC characteristics that is beyond the two-mode approximation.

The finite lifetime of BEC in the trap and of Rabi oscillations' coherence sets limits to the available time of experiments. If this requirement is satisfied, then justified is also the neglect of noise-induced switching between different regimes of the nonlinear Rabi oscillations presented above. Taking into account the progress in techniques of the BEC trapping and low-noise micromechanics, we believe in the reliability of an experimental demonstration of high sensitivity of conservative nonlinear Rabi oscillations to initial conditions, as shown above. Even if a number of states are initially populated, it is possible to select just a pair of them by the proper choice of modulation frequency. Note also that one can vary the initial populations of the resonant levels by an additional pulse of microwave radiation with carrier frequency close to the resonance. Similar phenomena are expected to exist in other nonlinear driven quantum systems including semiconductors, quantum dots, and superconducting devices.

ACKNOWLEDGMENTS

The author is very grateful to N. V. Vyssotina for the numerical simulation and to E. A. Ostrovskaya, Yu. V. Rozhdestvenskii, and G. B. Sochilin for helpful discussions. This study is supported by the Program of the Russian Academy of Sciences “Fundamental problems of nonlinear dynamics in mathematical and physical sciences” and by the University ITMO grant.

- [1] L. Allen and J. H. Eberly, *Optical Resonance and Two-Level Atoms* (Dover, New York, 1987).
 [2] M. O. Scully and M. S. Zubairy, *Quantum Optics* (Cambridge University Press, Cambridge, 1997).

- [3] F. Rossi and T. Kuhn, *Rev. Mod. Phys.* **74**, 895 (2002).
 [4] P. N. Romanets and F. T. Vasko, *Phys. Rev. B* **81**, 241411(R) (2010).

- [5] E. S. Andrianov, A. A. Pukhov, A. V. Dorofeenko, A. P. Vinogradov, and A. A. Lisyansky, *Phys. Rev. B* **85**, 035405 (2012).
- [6] M. R. Matthews, B. P. Anderson, P. C. Haljan, D. S. Hall, M. J. Holland, J. E. Williams, C. E. Wieman, and E. A. Cornell, *Phys. Rev. Lett.* **83**, 3358 (1999).
- [7] K. R. Patton and U. R. Fischer, *Phys. Rev. A* **87**, 052303 (2013).
- [8] Y. Chang, T. Shi, Y. X. Liu, C. P. Sun, and F. Nori, *Phys. Rev. A* **83**, 063826 (2011).
- [9] T. J. Alexander, K. Heenan, M. Salerno, and E. A. Ostrovskaya, *Phys. Rev. A* **85**, 063626 (2012).
- [10] M. M. Dos Santos, T. Oniga, A. S. Mcleman, M. Caldwell, and C. H.-T. Wang, *J. Plasma Phys.* **79**, 437 (2013).
- [11] A. I. Baz', Ya. B. Zeldovich, and A. M. Perelomov, *Scattering, Reactions and Decay in Nonrelativistic Quantum Mechanics*, Engl. Israel Program for Scientific Publications, Jerusalem, 1969 (Nauka, Moscow, 1971).
- [12] N. N. Rosanov and G. B. Sochilin, *JETP* (to be published).
- [13] L. D. Landau and E. M. Lifshitz, *Quantum Mechanics* (Pergamon Press, Oxford, 1977).
- [14] L. P. Pitaevskii and S. Stringari, *Bose-Einstein Condensation* (Clarendon Press, Oxford, 2003).
- [15] S. A. Moskalenko and D. W. Snoke, *Bose-Einstein Condensation of Excitons and Biexcitons and Coherent Nonlinear Optics with Excitons* (Cambridge University Press, Cambridge, 2000).
- [16] B. M. Caradoc-Davies, R. J. Ballagh, and K. Burnett, *Phys. Rev. Lett.* **83**, 895 (1999).